XLIII CILAMCE
21–25, November, 2022
FOZ DO IGUAÇU – PR – BRAZIL

Formulation for the local contact problem between smooth convex NURBS particles

Marina V. Craveiro[1], Alfredo Gay Neto[1]

[1]*Department of Structural and Geotechnical Engineering, Polytechnic School at University of São Paulo*
Av. Prof. Almeida Prado, trav. 02, nº 83, 05508-070, São Paulo, SP, Brazil
marina.craveiro@usp.br, alfredo.gay@usp.br

Abstract. The paper presents a formulation for the local contact problem between smooth convex particles whose boundaries are defined by a set of non-uniform rational B-splines surfaces. By assuming a master-to-master approach for the contact and an optimization scheme, the maximum penetration between particles is a minimum of an objective function that gives a constrained distance between surfaces. This objective function is defined with the aid of the Minkowski sum, configuration space obstacle and support mapping, which are concepts usually employed on computer graphics. A numerical example shows the good behavior of the method in handling contact between generic particle shapes. Comments on the numerical problems that can arise when generating particle boundaries with multiple patches are also presented.

Keywords: computer graphics, contact, discrete element method, NURBS.

1 Introduction

The discrete element method (DEM) can be used to study the mechanical behavior of particle systems. DEM was introduced by Cundall and Strack [1], and it describes the motion of each particle by the Newton-Euler equations. The interaction between particles is due to contact and, therefore, the method is extremely dependent on their geometry. More realistic geometries lead to better responses concerning the overall system behavior. However, the contact detection between complex geometries can be a hard-working task that demands high computing power. Precision and efficiency must then be balanced, which directly influences the choice of particle geometric features.

Spheres, ellipsoids, superellipsoids, polyhedra, cluster and clump of spheres are common geometric simplifications employed in DEM simulations. Song *et al*. [2], for instance, use spheres to model particles. He *et al*. [3] perform simulations with ellipsoids. Wellmann, Lillie and Wriggers [4] work with superellipsoids. Gay Neto and Wriggers [5], in their turn, analyze polyhedral systems. Finally, cluster and clump of spheres are studied by Li and McDowell [6]. Another possible mathematical representation for the particle boundary is the non-uniform rational B-splines (NURBS). They are very common in computer aided design (CAD), computer graphics and isogeometric analysis (IGA), but only recently they have been used in DEM simulations. Lim, Krabbenhoft and Andrade [7], Liu *et al*. [8] and Craveiro, Gay Neto and Wriggers [9] can be cited in this context.

According to Wriggers and Avci [10], the contact detection is the main responsible for the efficiency of DEM simulations. So, it is usual to divide the process into local and global levels. The latter involves low-cost computational algorithms to eliminate improbable contact pairs, and the former uses more precise algorithms, which vary with particle geometry, to determine if the particles are in contact and, if so, which are the contact points and the corresponding gap or penetration. The local search for contact is applied only to pairs of particles found by the previous global search, and it is herein named as local contact problem (LCP).

There are several techniques to solve contact. Lu, Third and Müller [11] present a review of contact detection between usual geometries. For more general ones and assuming a local quadratic approximation for surfaces, Gay Neto and Wriggers [12] treat the LCP as an optimization scheme. It is able to both detect contact and find the maximum penetration, which is a saddle point of the objective function. Concerning NURBS, Lim and Andrade

[13] use an intersection-based approach to study the contact between convex surfaces. Lim, Krabbenhoft and Andrade [7], in their turn, deal with non-convex NURBS using a master-to-slave contact formulation.

The contact issue is not a concern only of computational mechanics. Computer graphics also deals with it, requiring fast processes. The Gilbert–Johnson–Keerthi (GJK) distance algorithm and the expand polytope algorithm (EPA) are examples of contact algorithms. Details can be found in Ericson [14] and van den Bergen [15]. Little exchange, however, can be found between both areas.

Regarding the previous scenario, the objective of the work is to present a formulation for the LCP between smooth convex NURBS particles using a master-to-master contact approach, i.e., no contact points are chosen *a priori*. This approach, by the authors' knowledge, has not been applied to NURBS yet. The formulation determines the maximum penetration between contacting particles, which is the basic quantity to evaluate the contact forces to be considered in the Newton-Euler equations. The contact detection is done previously by the algorithm given in Gay Neto and Wriggers [12]. In the same way as these authors, the maximum penetration is determined by an optimization scheme. However, this quantity is herein a minimum and not a saddle point. It is possible by using computer graphics concepts. The LCP formulation is implemented into the software *Giraffe* [16], which also allows us to perform DEM simulations. The NURBS surfaces are created in the software *Rhinoceros 3D* [17].

2 Modeling particles with non-uniform rational B-splines (NURBS)

General surfaces can be mathematically defined by NURBS. The rational function

$$\boldsymbol{s}(u,v) = \frac{\sum_{i=0}^{n}\sum_{j=0}^{m} N_{i,p}(u)N_{j,q}(v)w_{i,j}\boldsymbol{p}_{i,j}}{\sum_{i=0}^{n}\sum_{j=0}^{m} N_{i,p}(u)N_{j,q}(v)w_{i,j}} \tag{1}$$

maps two parameters u and v into material points $\mathbf{s}(\mathrm{u},\mathrm{v})$ on surfaces, where $\mathrm{N_{i,p}(u)}$ and $\mathrm{N_{j,q}(v)}$ are piecewise polynomial basis functions with degrees p and q, $\mathbf{p}_{\mathrm{i,j}}$ are control points, $\mathrm{w_{i,j}}$ are weights, $\mathrm{n}+1$ and $\mathrm{m}+1$ are the number of control points associated with u and v, respectively. Details on NURBS can be found in Piegl and Tiller [18].

Naming patch as a parameterization of a surface region, one can model the particle closed boundary with either only one or more patches. The first option leads to poles and seam on the surface, as depicted in Fig. 1a. Poles consist in material points associated with multiple pairs of parameters u and v. They imply null derivatives with respect to one of such parameters, which is undesirable in numerical processes. The seam, in its turn, defines at the same curve the beginning and the end of the parametric space in direction u or v. So, one has to properly handle the change of parameters. Modeling closed surfaces using multiple patches eliminates poles, as can be seen in Fig. 1b. The seam issue remains, but it is modified. It is not necessary to change parameters within the patch itself, but to change parameters between patches. The present work chose to model particles with multiple patches. It is important to advice that this strategy also presents problems, especially because the focus herein is on smooth convex particles. The connections between the patches are not always perfect and smooth. They can have geometric imperfections whose treatment is not straightforward. These imperfections are not scope of the paper.

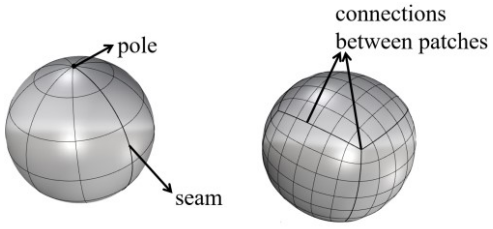

Figure 1. Modeling NURBS particles with (a) one patch (b) multiple patches

3 Computer graphics

Three computer graphics concepts need to be introduced in order to develop the LCP formulation: Minkowski sum, configuration space obstacle (CSO) and support mapping.

Consider two convex bodies A and B. The Minkowski sum A + B is the sum of all points $\mathbf{x}_A$ belonging to A with all points $\mathbf{x}_B$ belonging to B, as follows

$$A + B = \{\boldsymbol{x}_A + \boldsymbol{x}_B \mid \boldsymbol{x}_A \in A, \boldsymbol{x}_B \in B\}. \tag{2}$$

The CSO is the Minkowski sum $A + (-B)$, and it gives distances between bodies. The boundary representation of the CSO is the convex hull of the set $A + (-B)$. It is useful to check if the contact between A and B exists and, if so, to determine the maximum penetration. The contact exists if the CSO contains the origin, and the maximum penetration $d(A, B)$ is the minimum distance between the CSO boundary and its origin, as follows

$$d(A, B) = inf\ \{\|\boldsymbol{x}_{A-B}\| \mid \boldsymbol{x}_{A-B} \in A - B\}. \tag{3}$$

The support mapping is an implicit representation of a convex body geometry, which is defined as

$$\boldsymbol{d} \cdot \boldsymbol{map}(\boldsymbol{d}) = max\ \{\boldsymbol{d} \cdot \boldsymbol{x}_w \mid \boldsymbol{x}_w \in W\}. \tag{4}$$

Given a direction $\mathbf{d}$ and a body W, it returns $\mathbf{map}(\mathbf{d})$, which is a point $\mathbf{x}_W$ whose dot product with $\mathbf{d}$ is maximum, i.e., the furthest point $\mathbf{x}_W$ along that direction. For smooth bodies, the external normal of the body at $\mathbf{x}_W$ is parallel to $\mathbf{d}$.

The support mapping can be used to obtain points on the CSO boundary. For a given direction $\mathbf{d}$,

$$\boldsymbol{map}_{A-B}(\boldsymbol{d}) = \boldsymbol{map}_A(\boldsymbol{d}) - \boldsymbol{map}_B(-\boldsymbol{d}), \tag{5}$$

which results from the application of two support mappings, one for each body to which the CSO refers. See Fig. 2 for the geometric description of the support mapping. Note that, as we can find points on the CSO boundary, we can minimize the distance of these points to the origin, which results in the maximum penetration between bodies.

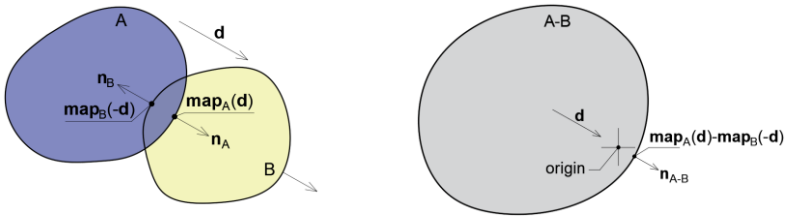

Figure 2. Description of the support mapping for intersecting bodies A and B

4 Local contact problem (LCP)

Consider two convex particles modeled with multiple NURBS patches. If contact is established between them, only one pair of contacting points is to be found by a master-to-master contact approach. A strategy to detect such points is to test each patch of one particle against each patch of the other. As commented, efficiency can be improved by previously employing global contact search algorithms, such as bounding volumes, in order to eliminate pairs of patches that have no chance of contact. Consequently, the LCP will be solved only for those pairs of patches whose interaction is probable.

Consider surfaces $\Gamma_A = \hat{\Gamma}_A(\zeta_A, \theta_A)$ and $\Gamma_B = \hat{\Gamma}_B(\zeta_B, \theta_B)$, whose parametrizations assume the form

$$\Gamma(\zeta, \theta) = \boldsymbol{x_0} + \boldsymbol{Q_0 s}(\zeta, \theta), \tag{6}$$

where ζ and θ are parameters (e.g., parameters u and v of NURBS), $\mathbf{x}_0$ represents a translation and $\mathbf{Q}_0$ a rotation tensor. They represent patches of particles. For a frozen configuration of the system, defining the gap vector $\mathbf{g}$ as

$$\boldsymbol{g} = \Gamma_A - \Gamma_B, \tag{7}$$

one may verify if two surfaces are in contact by minimizing the objective function

$$f_1 = \frac{1}{2}\|\boldsymbol{g}\|^2 = \frac{1}{2}\|\Gamma_A(\zeta_A, \theta_A) - \Gamma_B(\zeta_B, \theta_B)\|^2 \tag{8}$$

that defines the distance between them, as proposed by Gay Neto and Wriggers [12]. If the minimization leads to $f_1 > 0$, there is no contact between the surfaces, and their distance is $\|\mathbf{g}\|$. If $f_1 = 0$, the surfaces are intersecting each other, and the maximum penetration is a saddle point of f_1. The variables are the four convective coordinates.

It is possible to avoid the search for saddle points, which is not so straightforward as searching for minima, by writing a new objective function f_2 based on the aforementioned computer graphics concepts. Since the CSO of surfaces Γ_A and Γ_B represents distances between them and the smallest distance between the CSO boundary and its origin is the maximum penetration, the idea is no longer to unrestrictedly minimize the distance between the two surfaces, but to minimize the distance between points on those surfaces that lead to the boundary of the CSO. For that, one may define the direction $\mathbf{d}$ in the CSO in a spherical coordinate system as

$$\boldsymbol{d} = \{cos\,\rho\,sin\,\varphi\,, sin\,\rho\,sin\,\varphi\,, cos\,\varphi\}, \tag{9}$$

where ρ and φ are the azimuth angle and the elevation angle, respectively. With that, f_2 can be written as

$$f_2 = \frac{1}{2}\|\boldsymbol{g}\|^2 = \frac{1}{2}\left\|\Gamma_A\big(\zeta_A(\rho,\varphi),\theta_A(\rho,\varphi)\big) - \Gamma_B\big(\zeta_B(\rho,\varphi),\theta_B(\rho,\varphi)\big)\right\|^2, \tag{10}$$

in which the variables are no longer the four convective coordinates, but the angles that define the direction $\mathbf{d}$ in spherical coordinates. So, the minimization of f_2 leads to the direction of maximum penetration. The corresponding points on the surfaces can be obtained by applying the support mapping to the surfaces with that direction. The direction of maximum penetration is parallel to the gap $\mathbf{g}$ and to the external normals of the surfaces at the corresponding points. Note that a common-normal approach is reached.

To minimize f_2, the trust-region Newton method is chosen. It approximates the objective function by a quadratic model and minimizes it within a region in which such approximation is acceptable. For that, the step-length on the variables at each iteration is constrained. The process advances for the next iteration only if the objective function reduces within the current iteration and if the ratio between the actual and the approximated reductions respects preestablished limits. Nocedal and Wright [19] describe the numerical method in depth.

Each iteration of the optimization process refers to a direction $\mathbf{d}$. To find the corresponding convective coordinates ζ_A, θ_A, ζ_B and θ_B, it is necessary to apply the support mapping to surfaces Γ_A and Γ_B. These support mappings can be understood as another minimization problems by changing the sign of eq. (4). The objective functions to be minimized are

$$f_{supA} = -\boldsymbol{d}\cdot\,\boldsymbol{map}_A(\boldsymbol{d}) = -\boldsymbol{d}\cdot\,\Gamma_A(\zeta_A,\theta_A) \text{ and } f_{supB} = +\boldsymbol{d}\cdot\,\boldsymbol{map}_B(-\boldsymbol{d}) = +\boldsymbol{d}\cdot\,\Gamma_B(\zeta_B,\theta_B) \tag{11}$$

for surfaces Γ_A and Γ_B, respectively. One may impose the stationary conditions

$$\nabla f_{supA} = \boldsymbol{o}_2 \text{ and } \nabla f_{supA} = \boldsymbol{o}_2, \tag{12}$$

respectively, to find the critical points.

Regardless the optimization method, one has to evaluate the gradient and the Hessian of the objective function f_2 for each iteration. Note that f_2 is dependent on the convective coordinates, which, in their turn, are dependent on the angles ρ and φ. So, f_2 is a composite function. By ordering the surface parameters as $\zeta_A = \eta_1$, $\theta_A = \eta_2$, $\zeta_B = \eta_3$ and $\theta_B = \eta_4$, the terms of the gradient and the Hessian of f_2 are

$$\frac{\partial f_2}{\partial \rho} = \frac{\partial f_2}{\partial \eta_i}\frac{\partial \eta_i}{\partial \rho}, \qquad \frac{\partial f_2}{\partial \varphi} = \frac{\partial f_2}{\partial \eta_i}\frac{\partial \eta_i}{\partial \varphi}, \tag{13}$$

$$\frac{\partial^2 f_2}{\partial \rho^2} = \frac{\partial^2 f_2}{\partial \eta_i^2}\left(\frac{\partial \eta_i}{\partial \rho}\right)^2 + \frac{\partial f_2}{\partial \eta_i}\frac{\partial^2 \eta_i}{\partial \rho^2}, \qquad \frac{\partial^2 f_2}{\partial \varphi^2} = \frac{\partial^2 f_2}{\partial \eta_i^2}\left(\frac{\partial \eta_i}{\partial \varphi}\right)^2 + \frac{\partial f_2}{\partial \eta_i}\frac{\partial^2 \eta_i}{\partial \varphi^2}, \tag{14}$$

$$\frac{\partial^2 f_2}{\partial \rho \partial \varphi} = \frac{\partial^2 f_2}{\partial \eta_i^2}\frac{\partial \eta_i}{\partial \rho}\frac{\partial \eta_i}{\partial \varphi} + \frac{\partial f_2}{\partial \eta_i}\frac{\partial^2 \eta_i}{\partial \rho \partial \varphi}. \tag{15}$$

The derivatives of the surfaces Γ_A and Γ_B with respect to their parameters are easily found by well-known algorithms described in Piegl and Tiller [18]. The derivatives of the surface parameters with respect to the angles ρ and φ, however, are not straightforward. They have to be obtained implicitly by differentiating eqs. (12) with respect to angles ρ and φ. The process results in the following linear systems

$$\frac{\partial\left(\nabla f_{supA}\right)}{\partial \rho} = \boldsymbol{o}_2 \text{ and } \frac{\partial\left(\nabla f_{supB}\right)}{\partial \rho} = \boldsymbol{o}_2, \tag{16}$$

$$\frac{\partial(\nabla f_{supA})}{\partial\varphi} = \boldsymbol{o}_2 \text{ and } \frac{\partial(\nabla f_{supB})}{\partial\varphi} = \boldsymbol{o}_2, \tag{17}$$

$$\frac{\partial^2(\nabla f_{supA})}{\partial\rho^2} = \boldsymbol{o}_2 \text{ and } \frac{\partial^2(\nabla f_{supB})}{\partial\rho^2} = \boldsymbol{o}_2, \tag{18}$$

$$\frac{\partial^2(\nabla f_{supA})}{\partial\varphi^2} = \boldsymbol{o}_2 \text{ and } \frac{\partial^2(\nabla f_{supB})}{\partial\varphi^2} = \boldsymbol{o}_2, \tag{19}$$

$$\frac{\partial^2(\nabla f_{supA})}{\partial\rho\partial\varphi} = \boldsymbol{o}_2 \text{ and } \frac{\partial^2(\nabla f_{supB})}{\partial\rho\partial\varphi} = \boldsymbol{o}_2. \tag{20}$$

An initial estimate for direction $\mathbf{d}$ is necessary to start the iterative process of minimizing f_2. A suggestion is to use information of the intersection point found by minimizing f_1. Thus, the initial direction $\mathbf{d}$ can be the vector subtraction of the external normals to the surfaces Γ_A and Γ_B at the intersection point.

Finally, it is worth mentioning that, if the surface parameters are out of their valid range during the optimization processes, it is possible to change patches by storing their connectivity information.

The complete description of algorithms can be found in Craveiro, Gay Neto and Wriggers [9].

Remark 1: Contact between particles and planes. When dealing with the contact between particles and planes, the LCP is simplified, because the direction of maximum penetration is already known. It is the normal of the plane. So, it is enough to apply the support mapping to the particle and to project the point found on the plane.

5 DEM simulation

The LCP formulation is tested with a DEM simulation involving two NURBS particles. The particles are modeled with six NURBS patches whose basis functions are cubic polynomials for both directions of the parametric space. They are rigid and convex. The properties are indicated in Tab. 1.

Table 1. Rigid body data and initial conditions of NURBS particles

Particle	Mass (kg)	Inertia tensor **J** (kg.m^2)	$\mathbf{x}_0$ (m)	$\mathbf{Q}_0$
A	0.4874	$\begin{bmatrix} 1.0292 & -0.0361 & 0.0243 \\ -0.0361 & 0.9332 & 0.0915 \\ 0.0243 & 0.0915 & 0.7996 \end{bmatrix}.10^{-7}$	(0, 0, 0.26)	$\begin{bmatrix} 1 & 0 & 0 \\ 0 & 1 & 0 \\ 0 & 0 & 1 \end{bmatrix}$
B	0.4619	$\begin{bmatrix} 0.7675 & 0.0000 & 0.0000 \\ 0.0000 & 0.7862 & 0.0000 \\ 0.0000 & 0.0000 & 1.1259 \end{bmatrix}.10^{-7}$	(0.018, 0.015, 0.330)	$\begin{bmatrix} 1 & 0 & 0 \\ 0 & 1 & 0 \\ 0 & 0 & 1 \end{bmatrix}$

***** **J** is provided with respect to local barycentric axes

The simulation is performed with the aid of the software *Giraffe* [16], which deals with rigid bodies and has a master-to-master contact structure based on Gay Neto and Wriggers [20]. The contact is enforced by the penalty method, with normal penalty parameter $\epsilon_n = 10^8$ N/m and tangential penalty parameter $\epsilon_t = 10^7$ N/m. Damping is considered for contact both between particles and between particle and plane, with normal damping parameter $c_n = 10^5$ N.s/m. The Coulomb's friction model is assumed to rule the tangential interaction between bodies. The coefficient of friction is 0.3. The equations of motion are integrated over time by the Newmark implicit method. The total time of the simulation is 3 s. The initial time step is 0.001 s. See Gay Neto and Wriggers [20] for complete formulations.

At time t = 0 s, the particles are released from a certain height onto a plane located at coordinates (0,0,0.2). Under gravity, with magnitude 9.81 m/s^2, the particles first contact each other before contacting the plane. The initial configuration of the system is illustrated in Fig. 3 as well as the main configurations related to contact events.

After the initial collisions, which dissipate energy of the system, the movement of the particles on the plane is predominantly characterized by rolling, with no sliding. As the Coulomb's limit is not reached and no other sources of energy dissipation are considered in the model, no energy dissipation occurs at this stage of the simulation. Fig. 4 shows the system energy over time.

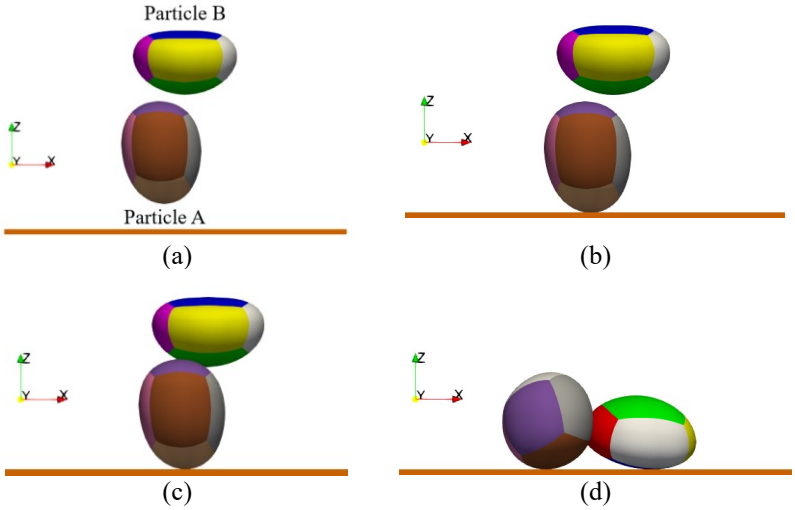

Figure 3. System configurations at (a) t = 0 s (b) 0.065 s (c) 0.07963 s (d) 0.21769 s

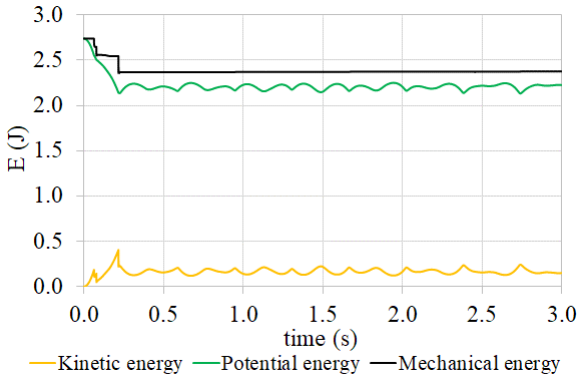

Figure 4. System energy over time

Observe that the proposed LCP formulation properly captures the mechanical behavior of the particle system, in view of the assumptions made.

6 Conclusions and future works

The present paper described the LCP formulation between NURBS particles in the context of a master-to-master contact approach. Using concepts from computer graphics and an optimization scheme, it is possible to determine the maximum penetration between contacting particles as a minimum of an objective function based on a constrained distance. A numerical example, in which the particles are modeled with multiple NURBS patches, showed that the formulation is able to deal robustly with the contact between generic smooth convex surfaces, capturing the expected qualitative mechanical behavior of the system.

Despite the robustness of the method, it is important to highlight that its computational cost still needs to be tested and optimized. This is because the method involves the solution of two optimization problems: the main problem of searching for maximum penetration and the application of support mappings to surfaces at each iteration of the main scheme. The iterative solution of these problems are cumbersome processes. The greater the

number of particles, the higher the computational cost. So, larger systems still have to be investigated.

Another point to be commented is that the method is developed based on concepts of computer graphics that are valid for convex shapes. So, the generation of the particle geometry must be perfect, without imperfections. In practice, this is not always possible with multiple patches. The connection between them, mainly the connection between three patches, may have local geometric imperfections, such as local concavities. At such regions, the LCP may fail, interrupting the numerical process. A possibility to overcome undesirable stops of DEM simulations is to impose points at the connections between patches to be candidate to contact. With that, there is a reduction of the number of variables of the LCP. This is very similar with the procedure named as degeneration by Gay Neto and Wriggers [21]. As future works, the idea is to deal with both local imperfections and imposed singularities at the connection between patches through degeneration technique.

Acknowledgements. The second author acknowledges CNPq (Conselho Nacional de Desenvolvimento Científico e Tecnológico) for the financial support under the research grant 304321/2021-4.

Authorship statement. The authors hereby confirm that they are the sole liable persons responsible for the authorship of this work, and that all material that has been herein included as part of the present paper is either the property (and authorship) of the authors, or has the permission of the owners to be included here.

References

[1] P.A. Cundall, O.D.L. Strack, A discrete numerical model for granular assemblies, *Géotechnique*. 29 (1979) 47–65. https://doi.org/10.1680/geot.1979.29.1.47.
[2] W. Song, B. Huang, X. Shu, J. Stránský, H. Wu, Interaction between railroad ballast and sleeper: a DEM-FEM approach, *Int. J. Geomech*. 19 (2019) 1–10. https://doi.org/10.1061/(ASCE)GM.1943-5622.0001388.
[3] S. He, J. Gan, D. Pinson, A. Yu, Z. Zhou, A discrete element method study of monodisperse mixing of ellipsoidal particles in a rotating drum, *Ind. Eng. Chem. Res.* 59 (2020) 12458−12470. https://doi.org/10.1021/acs.iecr.9b06623.
[4] C. Wellmann, C. Lillie, P. Wriggers, A contact detection algorithm for superellipsoids based on the common-normal concept, *Eng. Comput.* (Swansea, Wales). 25 (2008) 432–442. https://doi.org/10.1108/02644400810881374.
[5] A.G. Neto, P. Wriggers, Discrete element model for general polyhedra, *Comput. Part. Mech.* (2021). https://doi.org/10.1007/s40571-021-00415-z.
[6] H. Li, G.R. McDowell, Discrete element modelling of under sleeper pads using a box test, *Granul. Matter*. 20 (2018) 1–12. https://doi.org/10.1007/s10035-018-0795-0.
[7] K.W. Lim, K. Krabbenhoft, J.E. Andrade, On the contact treatment of non-convex particles in the granular element method, *Comput. Part. Mech*. 1 (2014) 257–275. https://doi.org/10.1007/s40571-014-0019-2.
[8] S. Liu, F. Chen, W. Ge, P. Ricoux, NURBS-based DEM for non-spherical particles, *Particuology*. 49 (2020) 65–76. https://doi.org/10.1016/j.partic.2019.04.005.
[9] M.V. Craveiro, A. Gay Neto, P. Wriggers, Contact between rigid convex NURBS particles based on computer graphics concepts, *Comput. Methods Appl. Mech. Eng*. 386 (2021) 114097. https://doi.org/10.1016/j.cma.2021.114097.
[10] P. Wriggers, B. Avci, Discrete element methods: basics and applications in engineering, in: *Model. Eng. Using Innov. Numer. Methods Solids Fluids*, Springer, Cham, 2020: pp. 1–30. https://doi.org/10.1007/978-3-030-37518-8_1.
[11] G. Lu, J.R. Third, C.R. Müller, Discrete element models for non-spherical particle systems: from theoretical developments to applications, *Chem. Eng. Sci.* 127 (2015) 425–465. https://doi.org/10.1016/j.ces.2014.11.050.
[12] A. Gay Neto, P. Wriggers, Numerical method for solution of pointwise contact between surfaces, *Comput. Methods Appl. Mech. Eng*. 365 (2020) 112971. https://doi.org/10.1016/j.cma.2020.112971.
[13] K.-W. Lim, J.E. Andrade, Granular element method for three-dimensional discrete element calculations, *Int. J. Numer. Anal. Methods Geomech*. 38 (2014) 167–188. https://doi.org/10.1002/nag.2203.
[14] C. Ericson, *Real-time collision detection*, 2005.
[15] G. van den Bergen, *Collision detection in interactive 3D environments*, CRC Press, 2003. https://doi.org/10.1201/9781482297997.
[16] A. Gay Neto, *Generic interface readily accessible for finite elements (Giraffe) – user's manual*, (2020).
[17] R. McNeel, *Rhinoceros 3D*, (2021). https://www.rhino3d.com/.
[18] L. Piegl, W. Tiller, *The NURBS Book*, Springer Berlin Heidelberg, Berlin, Heidelberg, 1995. https://doi.org/10.1007/978-3-642-97385-7.
[19] J. Nocedal, S.J. Wright, *Numerical optimization*, Springer New York, 2006. https://doi.org/10.1007/978-0-387-40065-5.
[20] A. Gay Neto, P. Wriggers, Master-master frictional contact and applications for beam-shell interaction, *Comput. Mech*. 66 (2020) 1213–1235. https://doi.org/10.1007/s00466-020-01890-6.
[21] A. Gay Neto, P. Wriggers, Computing pointwise contact between bodies: a class of formulations based on master–master approach, *Comput. Mech*. 64 (2019) 585–609. https://doi.org/10.1007/s00466-019-01680-9.